Multi-Agent Pattern Generation Using Unicycles

A Thesis
by

Soham Sachin Purohit
(Roll No. 190100117)

Supervisors:
Prof. Anirban Guha
and
Prof. Arpita Sinha

Department of Mechanical Engineering
Indian Institute of Technology Bombay
Mumbai 400076 (India)

3 May 2023

Declaration

I declare that this written submission represents my ideas in my own words and where others' ideas or words have been included, I have adequately cited and referenced the original sources. I declare that I have properly and accurately acknowledged all sources used in the production of this report. I also declare that I have adhered to all principles of academic honesty and integrity and have not misrepresented or fabricated or falsified any idea/data/fact/source in my submission. I understand that any violation of the above will be a cause for disciplinary action by the Institute and can also evoke penal action from the sources which have thus not been properly cited or from whom proper permission has not been taken when needed.

Soham Sachin Purohit

Date: 3 May 2023 (Roll No. 190100117)

Abstract

This work expanded on our previous project of generating patterns using a pair of unicycles. In this work, we developed a methodology for generating patterns using multiple agents with the same velocity following one or several other agents through a range-only control law validated using simulations. When extending the work in cases where the velocities were unequal, we tried multiple methods to obtain successful results but faced several challenges.

Table of Contents

List of Figures

List of Tables

Chapter 1

Introduction

In the context of using hypotrochoids for patrolling, coverage, and exploration, there exists a lot of work on single autonomous agents using linear, unicycle, and double integrator kinematic models to generate a wide variety of patterns. Different methods and control laws are employed to customize the trajectories to make them suited for different applications. In all these instances, employing multiple coordinated agents to perform this task is often considered advantageous over a single agent because it allows for a larger coverage area, a larger field of view, and a higher rate of acquiring information. This has led to several works on the 'formation control problem'.

A few methods employed in the formation control problem include generalizing the cyclic pursuit control scheme, Hopf oscillators for multi-agent systems, consensus protocols, and the modified and improved versions. All of these are intricate mathematical methods. There exists a need for a simplistic approach to the multi-agent pattern generation problem, which is the goal of this project.

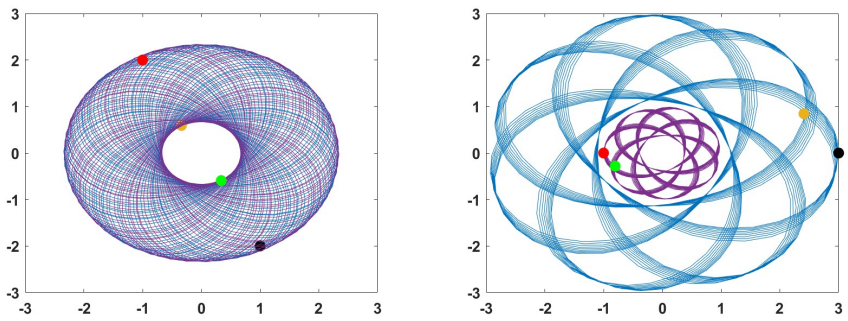

(a) (b)

Figure 1.1: Patterns generated by a pair of unicycles with a) Equal b) Unequal velocities

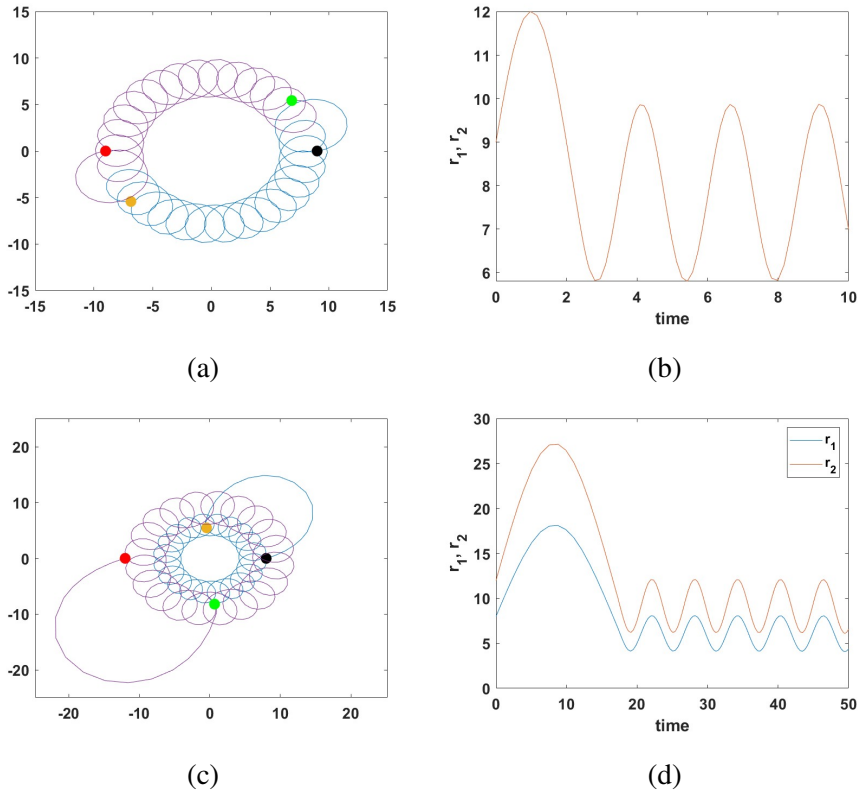

(a) (b)

(c) (d)

Figure 1.2: Trajectories and their r vs t graphs for the switching law

Our previous work expanded on Tripathy and Sinha (2018),Tripathy and Sinha (2016), and Tripathy and Sinha (2013). These works propose a control scheme that only requires the range between the agent and the target point for generating patterns using a single agent having unicycle kinematics. The benefit of this control scheme is that it generates a hypotrochoid pattern for every initial condition and gains value. Further, the controller gain can be tuned to achieve various desired trajectories to patrol the target point. Lastly, since the control scheme only requires the range information, the minimal information reduces operational costs. We extended the pattern formation with a single unicycle (Tripathy and Sinha, 2018) to the pattern formation with two unicycles.

We first mathematically proved the existence of a stationary point about which the two unicycles revolve and the initial conditions of the dynamics necessary for the point to remain stationary. Fig. 1.1 shows two such patterns generated by the unicycles in the equal and unequal velocity cases. With this, we could generate a variety of appealing patterns of different forms. There was little control over the overall shape of these annular patterns. To restrict the motion of the unicycles within a user-defined range of distances, we proposed a switching control law that altered the gains that enabled the unicycles to move within a pre-defined R_{min} and R_{max}. Fig. 1.2 displays a case each for the equal and

unequal velocity cases and their respective r vs time graphs when the switching law is applied.

The goal of this project was to extend and generalize these ideas to any number of robots from the two robot case. We wish to prove the existence of a stationary point and identify the initial conditions necessary for the point to remain stationary in the a) equal velocity case, b) unequal velocity case. The contributions of the project are as follows:

- Proposed the existence of a stationary point for the multi agent case with the set of initial conditions necessary for the point to remain stationary
- Various proposals for the stationary point in the the unequal velocity case and approaches to try to find the existence of a stationary point

The paper is organized as follows: Chapter 2 presents an extensive literature review of a few of the previous works that were the motivation for this project. Chapter 3 introduces the equal velocity problem and the control law, proposes a stationary point, and proves conditions necessary to achieve these trajectories. Chapter 4 presents the various approaches tried in the unequal velocity case and the simulation results.

Chapter 2

Literature Survey

In this chapter, we highlight the work in a few previous papers that were the motivation behind this project. We first briefly discuss applications and other pattern-generation methods employed for the single as well as the multi-agent cases.

In Schopferer *et al.* (2018), trochoids have been used for path planning of fixed-wing unmanned aircraft in uncertain wind conditions. Zhou *et al.* (2016) and Xu *et al.* (2019) use trochoids for tool path generation for inspecting surfaces and material removal on a surface. Trochoids also find wide use in patrolling, coverage, and exploration. In Coombes *et al.* (2018), the problem of coverage of a fixed-wing UAV has been tackled by using an optimal polygon decomposition method. Employing multiple coordinated agents to perform this task is often considered advantageous over a single agent because it allows for a larger coverage area, a larger field of view, and a higher rate of acquiring information. There exists a lot of work on single agents using linear, unicycle, and double integrator kinematic models to generate a wide variety of patterns. In Monsingh and Sinha (2019), trochoidal patterns are generated by multiple agents with single-integrator kinematics using a generalized consensus strategy based on Tsiotras and Castro (2014) and Tsiotras and Reyes Castro (2013). In Parayil and Ratnoo (2019), trochoids are generated using an agent with unicycle dynamics having a control law with parameters that cause the dynamics to exhibit supercritical Andronov-Hopf bifurcation.

There also exists a lot of work on the formation control problem. Through Ansart and Juang (2020b), Ansart and Juang (2020a), and Juang (2013), Juang uses single-integrator kinematics to propose a generalization of the cyclic pursuit control scheme and its extension thereafter. In Ansart and Juang (2021), the generalized cyclic pursuit law is used to maintain a group of agents in an epicycle-like formation. Ramachandran and Juang (2021) uses a Hopf oscillator for the multi-agent system to improve the robustness as compared to the cyclic pursuit control scheme. Tsiotras and Reyes Castro (2011) uses an

extension of the standard consensus protocol for generating periodic and quasi-periodic patterns. Tripathy and Sinha (2018), Tripathy and Sinha (2016), and Tripathy and Sinha (2013) propose a control scheme that only requires the range between the agent and the target point for generating patterns using a single agent having unicycle kinematics. These works have been highlighted further ahead since these are the primary motivations behind the project. The benefit of this control scheme is that it generates a hypotrochoid pattern for every initial condition and gain values. Further, the controller gain can be tuned to achieve a wide variety of desired trajectories to patrol the target point. Lastly, since the control scheme only requires the range information, the minimal information leads to a reduced operational cost.

An application using range-only measurements is Boyinine *et al.* (2019), in which range-only measurements are used for the landing control of a UAV on a moving ship.

We now discuss the primary motivation in greater detail.

2.1 Guidance of an Autonomous Agent for Coverage Applications using Range Only Measurement

The paper Tripathy and Sinha (2013) was the first paper that addressed the problem of single-agent pattern generation using a range-only control scheme. It uses the simple control scheme of:

$$u(t) = kr(t) \tag{2.1}$$

$R_{\min}$ and $R_{\max}$ were determined for this control law given any initial conditions. Further, if $R_{\min}$ and $R_{\max}$ are given, the conditions necessary to cover this region of interest were determined. It was observed that for some values of the initial parameters, a circular trajectory was achieved by the unicycle whose radius depended upon the initial conditions. Finally, the effect of varying the initial parameters was studied and presented. Some simulations were displayed to validate the previous results.

2.2 Generating Patterns With a Unicycle

The reference Tripathy and Sinha (2016) addresses the problem of making a unicycle trace hypotrochoid-like patterns using a simple range-based control scheme. The scheme used in this paper is:

$$u(t) = \eta r^{\mu}(t) \tag{2.2}$$

It proves that with the given control scheme and any gain, the unicycle achieves a hypotrochoid pattern always. The patterns are characterized based on the minimum and

maximum distances achieved by the unicycle from the target point. Conditions are determined for when the unicycle achieves the minimum and maximum distance from the target point. Further, the paper also determines the controller gains necessary to achieve any hypotrochoid pattern as desired using a switching law, that is, a law that changes the controller gain from an initial to a final value at a predefined value of r to ensure that the pattern traced lies within a certain set of values. The paper also determines whether a pattern can be achieved by the unicycle based on turn-rate constraints imposed on the unicycle. Finally, the work is validated by presenting simulation results.

2.3 Unicycle With Only Range Input: An Array of Patterns

The reference Tripathy and Sinha (2018) is an extension and generalization of Tripathy and Sinha (2016). The objective is again to generate planar hypotrochoid patterns by a unicyclic autonomous agent using the general range-based control scheme-

$$u(t) = f(t) \tag{2.3}$$

The paper characterizes the trajectories into five types based on the control law, initial conditions, and the velocity of the unicycle. These five types determine the type of trajectory, whether a hypotrochoid is generated, or an unbounded spiral. For the cases where a hypotrochoid is produced, the paper provides a methodology to determine the minimum and maximum distance from the target point achieved by the unicycle. A methodology for designing control for producing annular trajectories is proposed. This includes designing the control law and a switching strategy, the combination of which, produces an annular trajectory confined within the desired minimum and maximum distance from the target point. Finally, the results are validated through simulations and some appealing trajectories are displayed along with their generating control functions.

Chapter 3

Analysis and Results

3.1 Problem Description

In this project, we consider the patterns generated by n robots patrolling a target point $\mathcal{T}$. The robots are labeled R_i where i goes from 1 to n, and their position in the coordinate frame is at (x_i, y_i). We use a control law that requires only the distance between the robot under consideration and one or more other robots (r_{ij} is the distance of the i-th robot from the j-th robot), which is the line-of-sight (LOS) distance of one robot from the other. Fig. 3.1 displays an example of this multi-robot case with four robots. Their velocities are denoted by v_i , α_i are their corresponding heading directions, r_i is the distance between $\mathcal{R}_i$ and $\mathcal{T}$, and $\mathcal{T}$ is the target point (assumed to be at the origin without loss of generality). We assume that the robots are modeled as unicycles and hence have the kinematics governed by the following equations-

$$\dot{x}_i(t) = v_i cos(\alpha_i),\ \dot{y}_i(t) = v_i sin(\alpha_i),\ \dot{\alpha}_i(t) = u_i(t) \tag{3.1}$$

where u_i is the input. We consider that the input only requires the range of the robot i from the subsequent robot, and hence, we consider the control designed as

$$u_i(t) = \eta r_{ij}^{\mu}(t), \quad i = 1, 2, ..., n \quad j = \begin{cases} i+1 & i < n \\ 1 & i = n \end{cases} \tag{3.2}$$

where $\eta \neq 0$ is the controller gain and μ is a positive constant. Simply put, each robot follows the subsequent robot while tracing the trajectories.

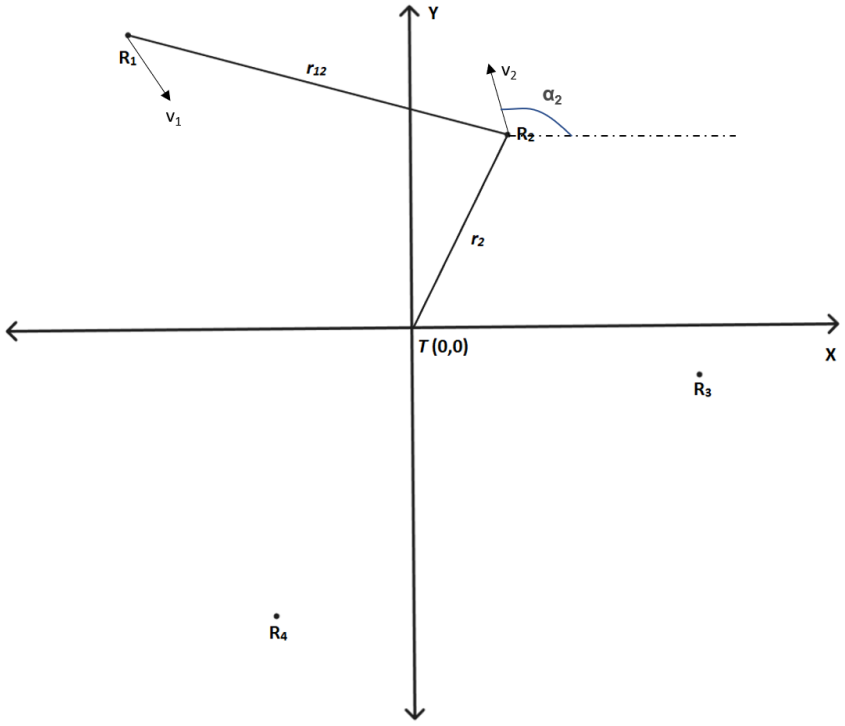

Figure 3.1: General setup of the problem with four robots $\mathcal{R}_i$ rotating about the stationary point $\mathcal{T}$ with only range r as input

3.2 Equal Velocities of All Robots

In the first section, we extend the ideas developed in the previous work to the case where all the robots have the same velocity. The extension is simple and yields positive results.

3.2.1 Trajectories of Interest

We want trajectories such that the robots have maximum coverage (remain at maximum distance from each other), and patrol a point that remains stationary. Without loss of generality, we assume that the point is at (0,0).

Proposition 1 *For the two robots with kinematics* (3.1) *following the control law* (3.8)*, the target point* $\mathcal{T}$ *remains at the geometric centroid of the n robots for all time if* $v_i = v_j$

$\forall$ i, j *and the initial conditions satisfy*

$$r_{ij0} = r_0 \quad j = i + 1 \tag{3.3}$$

$$\angle R_i R_{i+1} R_{i+2} = \frac{2\pi}{n} \tag{3.4}$$

$$\sum_{i=1}^{n} x_{i0} = 0; \sum_{i=1}^{n} y_{i0} = 0 \tag{3.5}$$

$$\alpha_{j0} = \alpha_{10} + \frac{2\pi(j-1)}{n}; \quad j > 1 \tag{3.6}$$

where (x_{i0}, y_{i0}) *and* α_{i0} *are the position and heading of robot* i *at the time* $t = 0$.

Proof: To prove that the target point, $\mathcal{T}$ = (0,0) remains at the centroid of the n robots for all times, we need to show that at $t = 0$, the centroid is at $\mathcal{T}$ and the rate of change of the position of the geometric centroid is zero at all times. Equation (3.5) establishes that the centroid at $t = 0$ is at (0,0). To show that the centroid remains constant for all time, let $x_m = (1/n)\sum_{i=1}^{n} x_i$, $y_m = (1/n)\sum_{i=1}^{n} y_i$ and $v_i = v$. We assume that each (x_i, y_i) satisfies (3.3) and (3.4), which implies that they form the vertices of a regular n-gon. From (3.1), (3.8), (3.3) and (3.4), we can see that because cyclic symmetry is maintained with symmetric initial conditions, $\dot{\alpha}_i = \dot{\alpha}_j$ for any i,j. Hence, we can write

$$\alpha_i(t) = F(t) + \alpha_{i,0}, \quad i = 1, 2, ..., n \tag{3.7}$$

where $F(t) = \int_0^t \eta r_{ij}^{\mu}(\tau) d\tau$, which is the same definite integral for all i,j through the argument made above. Now, from (3.1),

$$\dot{x}_m = \frac{v}{n}\left(\sum_{i=1}^{n} \cos\alpha_i\right) = \{\cos F(t)(\sum_{i=1}^{n} \cos\alpha_{i0}) - \sin F(t)(\sum_{i=1}^{n} \sin\alpha_{i0})\}\frac{v}{n}$$

$$\dot{y}_m = \frac{v}{n}\left(\sum_{i=1}^{n} \sin\alpha_i\right) = \{\sin F(t)(\sum_{i=1}^{n} \cos\alpha_{i0}) + \cos F(t)(\sum_{i=1}^{n} \sin\alpha_{i0})\}\frac{v}{n}$$

Applying (3.6), we see that both values go to 0 due to a trigonometric identity involving fractional values of 2π $\dot{x}_m = 0$ and $\dot{y}_m = 0$, implying that the centroid remains at $\mathcal{T}$ for all time. ■

Remark 1 *Note from the proof above that the control input need not just involve the robot following the subsequent robot. We can have any control input that is cyclically symmetric for all robots, which will let T remain stationary.*

The above remark implies that we have flexibility in the control input provided to each robot. We can use the robot's distance from other robots if the equation is cyclically symmetric for all robots. This can be useful when we want to dampen sensor noise, i.e., more sample points can effectively average out the noise.

	v	(x_{10}, y_{10})	(x_{20}, y_{20})	(x_{30}, y_{30})	α_{10}	α_{20}	α_{30}
Case a	10	(0,2.89)	(-2.5,-1.44)	(2.5,1.44)	30°	150°	270°
Case b	10	(0,0.58)	(-0.5,-0.29)	(0.5,0.29)	10°	130°	250°

Table 3.1: Three Robot Cases

	v	(x_{10}, y_{10})	(x_{20}, y_{20})	(x_{30}, y_{30})	(x_{40}, y_{40})	α_{10}	α_{20}	α_{30}	α_{40}
Case a	10	(1,1)	(-1,1)	(-1,-1)	(1,-1)	10°	100°	190°	280°
Case b	10	(0,1)	(-1,0)	(0,-1)	(1, 0)	30°	120°	210°	300°

Table 3.2: Four Robot Cases

3.2.2 Simulations and Results

To validate the results proved in the previous section, we run simulations for a three-robot and a four-robot case. First, we use a control input that makes each robot follow only the subsequent robot, validating Proposition 1.

Three robot case

The original control input is applied to the three robot cases with the following initial conditions. These initial conditions satisfy the conditions of Proposition 1-

The results of the simulations are shown in Fig. 3.2. a) and c) display the trajectories of the three robots. The red, black, and blue dots indicate the starting locations of the robots. We can see that the initial positions form an equilateral triangle in both cases. Graphs b) and d) display the X and Y coordinates of the centroid for each case. The centroid remains very close to 0 for the entire motion duration. This validates Proposition 1 in the three-robot case.

Four robot case

The simulations were repeated for the four-robot case. The two sets of initial conditions taken were:

The results of the simulations are shown in Fig. 3.3. a) and c) display the trajectories of the three robots. The red, black, blue, and green dots indicate the starting locations of the robots. We can see that the initial positions form a square in both cases. Graphs b) and d) display the X and Y coordinates of the centroid for each case. The centroid remains very close to 0 for the entire motion duration. This validates Proposition 1 in the four-robot case.

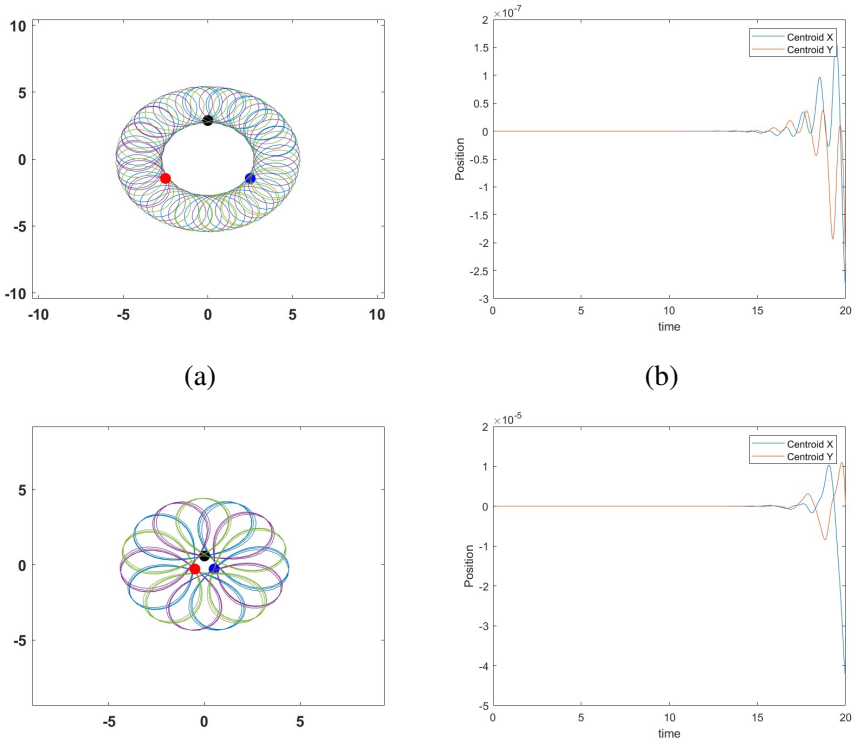

Figure 3.2: Three Robots, Equal Velocity

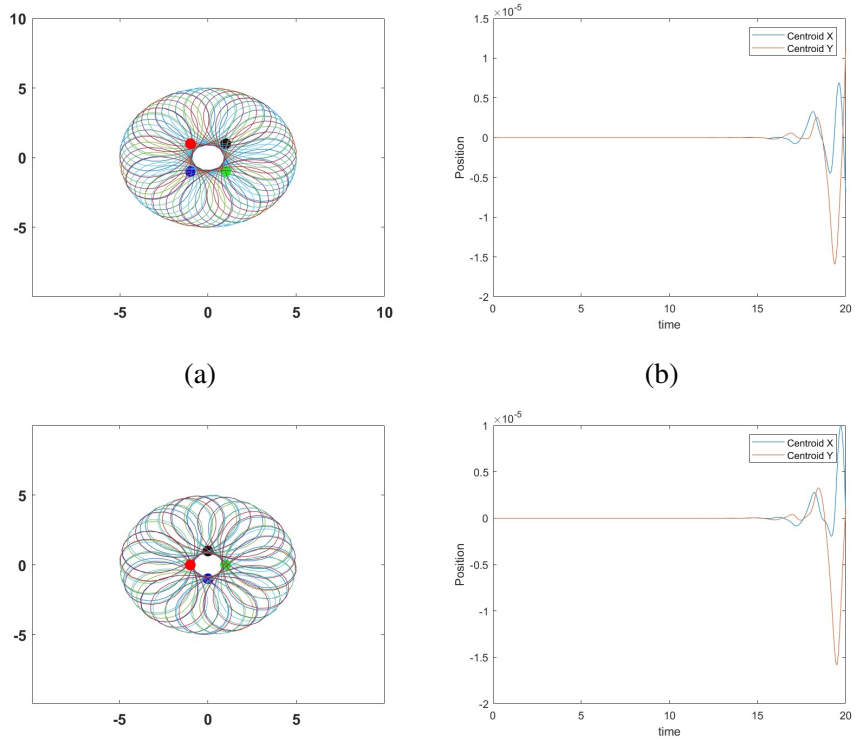

Figure 3.3: Four Robots, Equal Velocity

	v	η_1	η_2	(x_{10}, y_{10})	(x_{20}, y_{20})	(x_{30}, y_{30})	α_{10}	α_{20}	α_{30}
Case a	10	1	3	(0,2.89)	(-2.5,-1.44)	(2.5,1.44)	40°	160°	280°
Case b	10	0.5	5	(0,0.58)	(-0.5,-0.29)	(0.5,0.29)	60°	180°	300°

Table 3.3: Simulations for Remark 1

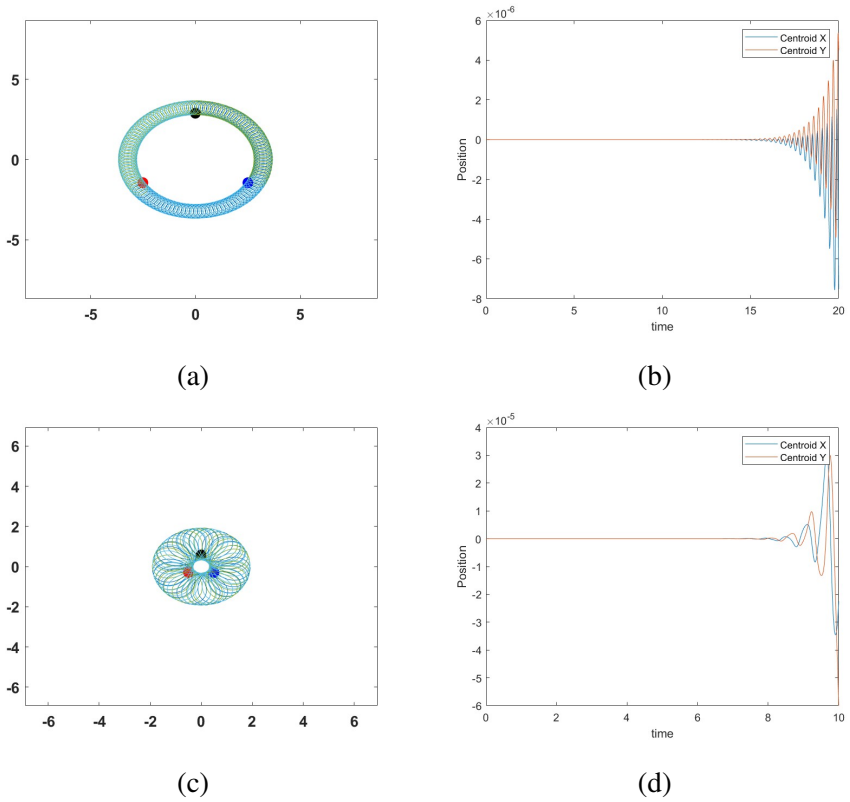

Figure 3.4: Simulations with a modified control law

Using other functions as Control

We now validate Remark 1 by simulating cyclically symmetric functions for the three-robot case of the form-

$$u_1(t) = \eta_1 r_{12}^{\mu}(t) + \eta_2 r_{13}^{\mu}(t); \quad u_2(t) = \eta_1 r_{23}^{\mu}(t) + \eta_2 r_{21}^{\mu}(t); \quad u_3(t) = \eta_1 r_{31}^{\mu}(t) + \eta_2 r_{32}^{\mu}(t) \quad (3.8)$$

The conditions of Proposition 1 remain the same. The two simulated cases are tabulated in Table 3.3.

The simulation results are displayed in Fig. 3.4. We again observe that the graphs of the centroids remain very close to $\mathcal{T}$ in both cases. This validates the stationarity of the centroid with the modified control law. This validates Remark 1.

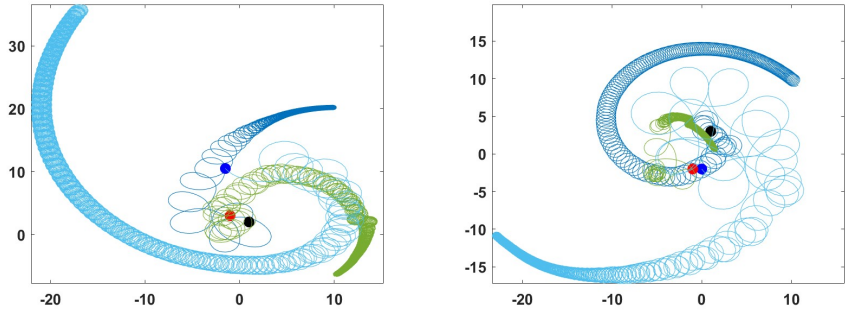

(a) (b)

Figure 3.5: Simulations with heading directions as proposed in Method 1

3.3 Unequal Velocities of Robots

Several methods were tried to extend the pattern generation about a stationary point, which, unfortunately, did not yield positive outcomes. The details of the methods are as follows:

3.3.1 Method 1

In the two-robot case, we hypothesized the existence of a stationary point and proved that the point, indeed, remained stationary for all future times. Here, we tried to extend the idea to the three-robot case directly.

For the unequal velocity two-robot case, the stationary point was given by-

$$x_f = \left(\frac{v_2}{v_1 + v_2}\right) x_1 + \left(\frac{v_1}{v_1 + v_2}\right) x_2 \tag{3.9}$$

$$y_f = \left(\frac{v_2}{v_1 + v_2}\right) y_1 + \left(\frac{v_1}{v_1 + v_2}\right) y_2 \tag{3.10}$$

Here, we first proposed that the stationary point would lie on either-

$$x_f = \left(\frac{v_2 v_3}{v_1 + v_2 + v_3}\right) x_1 + \left(\frac{v_1 v_3}{v_1 + v_2 + v_3}\right) x_2 + \left(\frac{v_1 v_2}{v_1 + v_2 + v_3}\right) x_3 \tag{3.11}$$

$$y_f = \left(\frac{v_2 v_3}{v_1 + v_2 + v_3}\right) y_1 + \left(\frac{v_1 v_3}{v_1 + v_2 + v_3}\right) y_2 + \left(\frac{v_1 v_2}{v_1 + v_2 + v_3}\right) y_3 \tag{3.12}$$

or

$$x_f = \left(\frac{v_2 v_3}{v_1 v_2 + v_2 v_3 + v_3 v_1}\right) x_1 + \left(\frac{v_1 v_3}{v_1 v_2 + v_2 v_3 + v_3 v_1}\right) x_2 + \left(\frac{v_1 v_2}{v_1 v_2 + v_2 v_3 + v_3 v_1}\right) x_3 \tag{3.13}$$

$$y_f = \left(\frac{v_2 v_3}{v_1 v_2 + v_2 v_3 + v_3 v_1}\right) y_1 + \left(\frac{v_1 v_3}{v_1 v_2 + v_2 v_3 + v_3 v_1}\right) y_2 + \left(\frac{v_1 v_2}{v_1 v_2 + v_2 v_3 + v_3 v_1}\right) y_3 \tag{3.14}$$

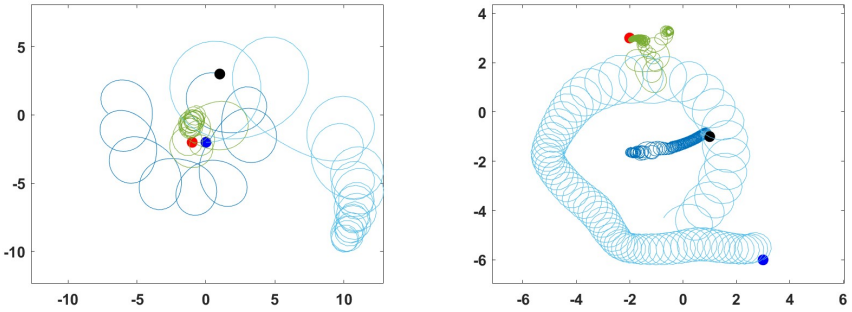

(a) (b)

Figure 3.6: Simulations with initial heading perpendicular to line joining proposed stationary point

In the two-robot case, the velocities of the robots were directly proportional to their distance from the stationary point. We now simulate trajectories that begin with the above point at $\mathcal{T}$ and the velocities in proportion to the distance of the initial point from the proposed stationary point. Since the initial conditions require the stationary point to be at (0,0) and the two proposed points differ only in their denominator, a lack of positive outcomes for the first also implies a lack of positive results for the second. Fig. 3.5 displays the simulation results. The trajectories do not have a stationary point and are also possibly unbounded. This invalidated our assumption of a fixed issue as proposed above. The reasoning behind this is the assumption we make in (3.7). Here, we cannot integrate α_i to be equal to a function F(t) for all the robots since there is no symmetry in the unequal robot case.

3.3.2 Method 2

Next, we decided to test whether the similarity of triangles was maintained if the initial heading direction was kept perpendicular to the line joining the vertex and the proposed stationary point. The results of the simulations are displayed in Fig. 3.6. Again, we see that the point does not remain stationary, proving the hypothesis false.

3.3.3 Method 3

In the previous section, we saw that a simplistic extension gives incorrect results. Next, we decided to check the following for the presence of a stationary point. Suppose the points formed by the three agents are such that the centroid of the triangle they formed lies at the origin. Suppose we provide velocities in proportion to their distance from the origin. If the initial heading direction is perpendicular to the line joining the agent and the

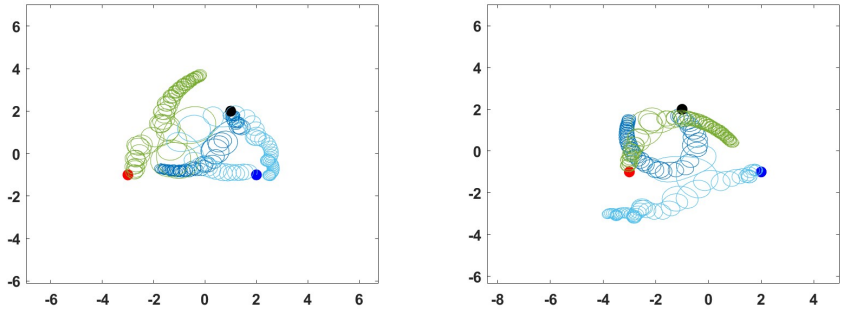

(a) (b)

Figure 3.7: Simulations with initial heading perpendicular to line joining median

centroid, would the centroid be stationary?
To do so, we determined the distance of the vertices from the centroid based on the lengths of the sides. The equations for the velocity ratios were as follows-

$$\frac{v_1}{v_2} = \sqrt{\frac{2r_{13}^2 + 2r_{12}^2 - r_{23}^2}{2r_{23}^2 + 2r_{12}^2 - r_{13}^2}} \tag{3.15}$$

$$\frac{v_2}{v_3} = \sqrt{\frac{2r_{23}^2 + 2r_{12}^2 - r_{13}^2}{2r_{23}^2 + 2r_{13}^2 - r_{12}^2}} \tag{3.16}$$

$$\frac{v_1}{v_3} = \sqrt{\frac{2r_{13}^2 + 2r_{12}^2 - r_{23}^2}{2r_{23}^2 + 2r_{13}^2 - r_{12}^2}} \tag{3.17}$$

Using these velocity ratios, simulations were run with the stationary point at the centroid of the triangle and the heading directions perpendicular to the line joining the vertex to the origin. The trajectories are displayed in Fig. 3.7. We again observe that the centroid does not remain stationary, contradicting the hypothesis.

Some more work is required to find the existence of a stationary point (if any) under certain conditions for the unequal velocity case

Chapter 4

Conclusion and Future Work

4.1 Conclusion

Through this project, we were able to extend a simple range-based control scheme for generating hypotrochoids from a double agent to a multi-agent case. Not only does this provide a simplistic methodology for generating patterns using multiple agents, but it also includes the advantages of using a range-only based control scheme, such as producing hypotrochoids for all values of the initial conditions and a reduced operational cost. While the extension of pattern generation to the multi-agent situation was straightforward for the equal velocity case, several challenges were faced in finding a stationary point when the velocities were not equal. At the heart of the problem lies the question of finding cyclic symmetry. Finding the answer to which initial conditions and velocities allow the Eq. 3.7 to be valid would help us determine the answer to multi-agent pattern generation about a stationary point.

4.2 Future Work

The first step would be to find the suitable conditions necessary to arrive at the existence of a stationary point in the three-agent case with unequal velocities. Following that, a generalization to multiple agents would give a recipe for generating patterns with any number of agents. Further, using a switching control law to restrict the distances of the agents from the stationary point, as was done for the two-agent case. Another possible solution in case initial conditions that allow the control law to be cyclically symmetric are not could be to develop a new algorithm that takes into account the varying velocities of the agents. This could involve developing a more complex mathematical model that can predict how the agents' velocities will affect the overall pattern.

References

Ansart, A., and Juang, J.-C., 2020a, "Generalized cyclic pursuit: A model-reference adaptive control approach," in *2020 5th International Conference on Control and Robotics Engineering (ICCRE)*, pp. 89–94.

Ansart, A., and Juang, J.-C., 2020b, "Generalized cyclic pursuit: An estimator-based model-reference adaptive control approach," in *2020 28th Mediterranean Conference on Control and Automation (MED)*, pp. 598–604.

Ansart, A., and Juang, J.-C., 2021, "Integral sliding control approach for generalized cyclic pursuit formation maintenance," *Electronics* **10**, doi:\bibinfo{doi}{10.3390/electronics10101217}

Boyinine, R., Chakraborty, A., Sharma, R., and Brink, K., 2019, "Development of sliding-mode landing controller using cooperative relative localization with pattern generation," in *2019 Sixth Indian Control Conference (ICC)*, pp. 128–133.

Coombes, M., Fletcher, T., Chen, W.-H., and Liu, C., 2018, "Optimal polygon decomposition for uav survey coverage path planning in wind," *Sensors* **18**

Juang, J.-C., 2013, "On the formation patterns under generalized cyclic pursuit," *IEEE Transactions on Automatic Control* **58**, 2401–2405.

Monsingh, J. M., and Sinha, A., 2019, "Trochoidal patterns generation using generalized consensus strategy for single-integrator kinematic agents," *European Journal of Control* **47**, 84–92.

Parayil, A., and Ratnoo, A., 2019, "Bifurcation-based control law for pattern generation," *IEEE Control Systems Letters* **3**, 374–379.

Ramachandran, K., and Juang, J.-C., 2021, "Application of oscillator dynamics for deviated pursuit formations: Preliminary results," in *2021 International Automatic Control Conference (CACS)*, pp. 1–6.

Schopferer, S., Lorenz, J. S., Keipour, A., and Scherer, S., 2018, "Path planning for unmanned fixed-wing aircraft in uncertain wind conditions using trochoids," in *2018 International Conference on Unmanned Aircraft Systems (ICUAS)*, pp. 503–512.

Tripathy, T., and Sinha, A., 2013, "Guidance of an autonomous agent for coverage applications using range only measurement," in *AIAA Guidance, Navigation, and Control (GNC) Conference*

Tripathy, T., and Sinha, A., 2016, "Generating patterns with a unicycle," *IEEE Transactions on Automatic Control* **61**, 3140–3145.

Tripathy, T., and Sinha, A., 2018, "Unicycle with only range input: An array of patterns," *IEEE Transactions on Automatic Control* **63**, 1300–1312.

Tsiotras, P., and Castro, L., 2014 01, "The artistic geometry of consensus protocols," ISBN 978-3-319-03903-9, pp. 129–153.

Tsiotras, P., and Reyes Castro, L. I., 2011, "Extended multi-agent consensus protocols for the generation of geometric patterns in the plane," in *Proceedings of the 2011 American Control Conference*, pp. 3850–3855.

Tsiotras, P., and Reyes Castro, L. I., 2013, "A note on the consensus protocol with some applications to agent orbit pattern generation," in *Distributed Autonomous Robotic Systems: The 10th International Symposium*, edited by Martinoli, A., Mondada, F., Correll, N., Mermoud, G., Egerstedt, M., Hsieh, M. A., Parker, L. E., and Støy, K. (Springer Berlin Heidelberg, Berlin, Heidelberg). ISBN 978-3-642-32723-0, pp. 345–358.

Xu, C.-Y., Li, J.-R., Liang, Y.-J., Wang, Q.-H., and Zhou, X.-F., 2019, "Trochoidal toolpath for the pad-polishing of freeform surfaces with global control of material removal distribution," *Journal of Manufacturing Systems* **51**, 1–16.

Zhou, Z., Zhang, Y., and Tang, K., 2016, "Sweep scan path planning for efficient freeform surface inspection on five-axis cmm," *Computer-Aided Design* **77**, 1–17.